

Supplemental materials:

Drug Concentration Asymmetry in Tissues and Plasma for Small Molecule-Related Therapeutic Modalities

Donglu Zhang, Cornelis ECA Hop, Gabriela Patilea-Vrana, Gautham Gampa, Herana Kamal Seneviratne, Jashvant D Unadkat, Jane R Kenny, Karthik Nagapudi, Li Di, Lian Zhou, Mark Zak, Matthew R Wright, Namandjé N Bumpus, Richard Zang, Xingrong Liu, Yurong Lai, S Cyrus Khojasteh

Table S1. Free drug concentration in tissue and plasma of selected drugs at pharmacokinetic steady state

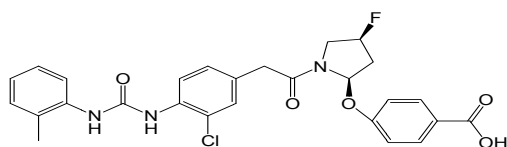
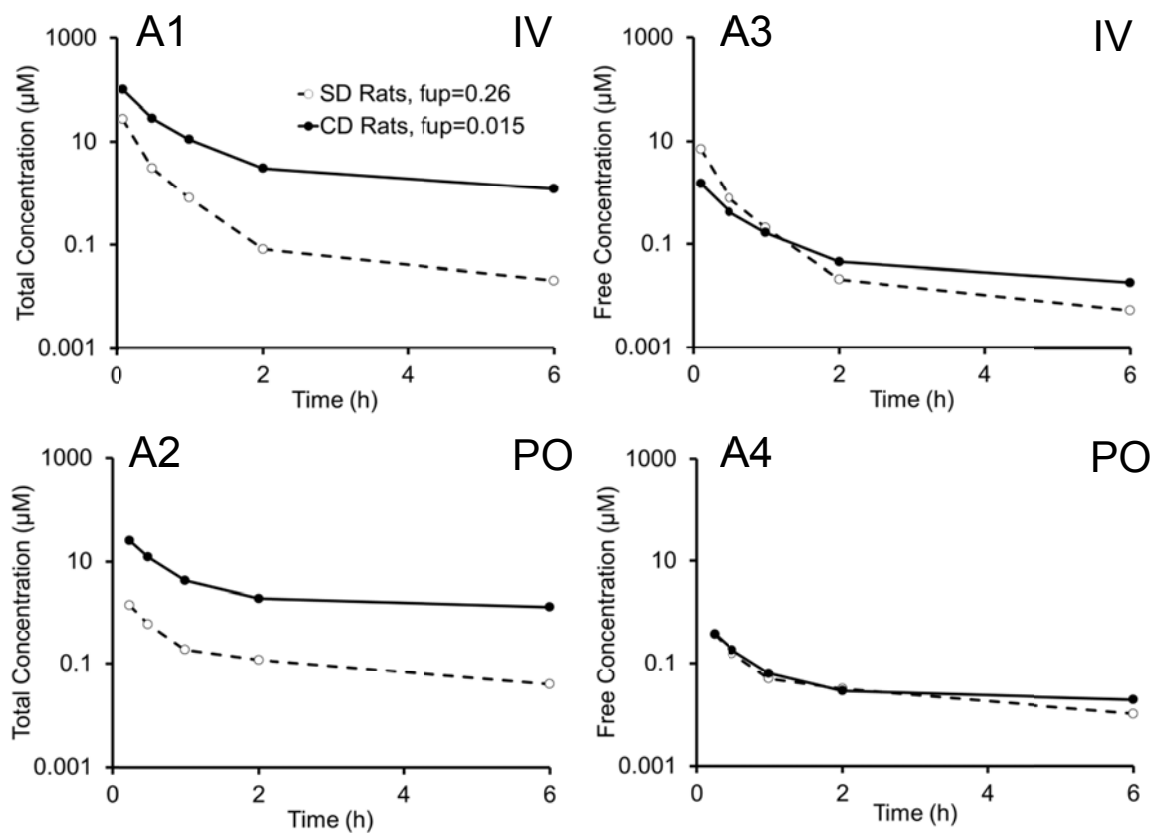
Free drug Concentration ($\mu\text{g/ml}$)	SY55551 (Deguchi et al., 1992)	Methotrexate (Ekstrom et al., 1996)	Cefminox (Deguchi et al., 1992)	Cefpodoxime (Liu et al., 2005)	Cefixime (Liu et al., 2005)
$C_{\text{plasma,u}}$	75 - 90	14.7	250	0.6*	0.3*
$C_{\text{liver,u}}$	64.2	17.6			
$C_{\text{lung,u}}$	68.7				
$C_{\text{muscle,u}}$	72.7	15.2		0.6*	0.3*
$C_{\text{adipose,u}}$			253		
*: $\text{AUC}_{0-24 \text{ h}}$					

Table S2. Determination of K_p and $K_{p,uu}$ of in vivo rat livers in vitro rat hepatocytes in media

Compounds	Concentration (ng/mL)		K_p		Plasma f_{up}	Liver $f_{u,liver}$ or $f_{u,cell}$	$f_{u,media}$	$K_{p,uu}$ In Vitro ^A	In Vivo	Fold Difference in Vivo $K_{p,uu}$ /in Vitro $K_{p,uu}$
	In Vivo Plasma	In Vivo Liver	In Vivo Liver to Plasma	In Vitro K_p^A						
Cerivastatin	261 ± 70	6717 ± 960	27 ± 8.0	27 ± 2.6	0.016 ± 0.001	0.017 ± 0.001	0.022 ± 0.003	21 ± 2.0	29 ± 8.5	1.4
Fluvastatin	245 ± 34	8990 ± 1490	37 ± 7.4	27 ± 1.8	0.011 ± 0.001	0.013 ± 0.001	0.016 ± 0.001	22 ± 1.5	44 ± 8.7	2.1
Rosuvastatin	14 ± 3.7	178 ± 50	13 ± 2.2	35 ± 0.6	0.044 ± 0.009	0.19 ± 0.02	0.19 ± 0.02	35 ± 0.6	57 ± 9.5	1.6
Pravastatin	33 ± 19	171 ± 15	6.7 ± 4.5	8.3 ± 0.8	0.54 ± 0.02	0.18 ± 0.02	0.49 ± 0.06	3.0 ± 0.3	2.2 ± 1.5	0.8
PF- 04991532	172 ± 67	1170 ± 364	7.1 ± 2.0	8.9 ± 0.1	0.12 ± 0.01	0.096 ± 0.02	0.12 ± 0.01	7.1 ± 0.1	5.7 ± 1.6	0.8
PF- 05187965	76 ± 21	323 ± 13	4.4 ± 1.0	10 ± 0.4	0.27 ± 0.01	0.15 ± 0.02	0.36 ± 0.01	4.2 ± 0.2	2.4 ± 0.57	0.6

A. In Vitro K_p rat hepatocytes and media with 4% BSA (Riccardi et al., 2016, 2017).

Figure S1. In Vivo effect of PPB on the total (A1 and A2) and free (A3 and A4) plasma concentration of compound D01-4582 in CD rats and SD rats. Its unbound fraction in CD rat and SD rat plasma was 0.015 and 0.26, respectively. Data is from Ito et al., 2007.



D01-4582

Figure S2: Figure S2: The distribution profiles of TFV, TFV-DP and phosphatidyl choline (PC, 16:0/OH) in colorectal tissue sections of four subjects. Research subjects (HIV-negative, men who have sex with men healthy volunteers (n=4)) received TFV enemas at two different time points (3 and 24 h) and two doses (low, 1.76 mg/mL in 125 mL and high, 5.28 mg/mL in 125 mL TFV concentrations). MALDI-MSI analysis was performed using colorectal biopsies and ion images (distribution profiles) were generated at a spatial resolution of 50 μ m. TFV and TFV-DP exhibited heterogeneous distribution across colorectal tissue sections whereas the localization of phosphatidyl choline (PC, 16:0/OH) was relative homogeneous. The highest signal intensity (100%) is represented by the red color whereas blue color depicts the lowest signal (0%) of the ion of interest. Scale bar, 1 mm. These data were published recently (Seneviratne et al., 2018).

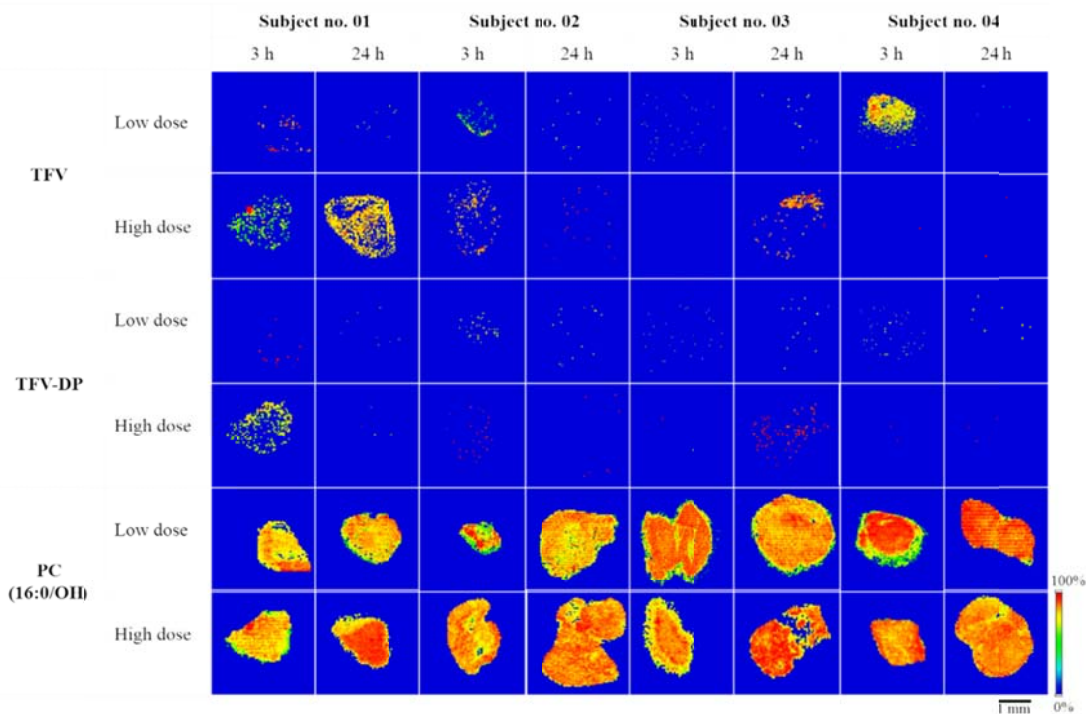


Figure S3. The schematic depicts multiple equilibrium processes that determine the drug distribution to the brain, the extent of drug distribution described by K_p and $K_{p,uu}$. The non-specific binding of a drug to components of plasma and brain can have a significant influence on K_p ; however, $K_{p,uu}$ is not confounded by non-specific drug binding and represents the true transport equilibrium across the BBB. BBB, blood–brain barrier; K_p , brain-to-plasma ratio; $K_{p,uu}$, unbound partition coefficient; f_u , unbound (free) fraction.

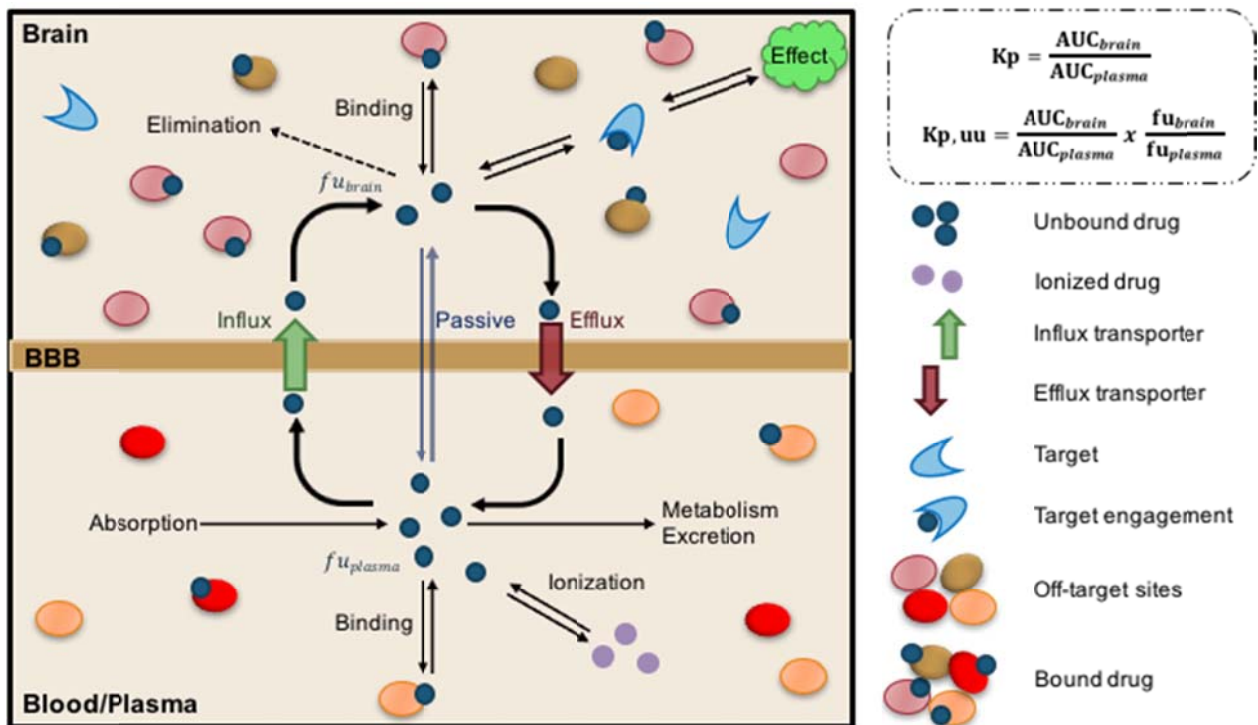


Figure S5. Types of NPs that have been investigated as therapeutics and diagnostics

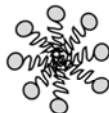
Inorganic Nanoparticles



Liposomes



Micelles



Dendrimers



Polymers

